RSC Advances

ROYAL SOCIETY OF CHEMISTRY

www.rsc.org/advances

Contents entry

1. Colour graphic:

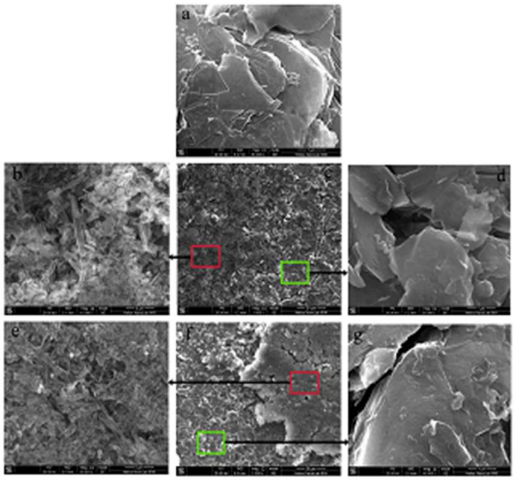

2. Text:

Phenomenon of lithium deposition in long-term cycled battery, effect on capacity loss of battery and mechanism of formation were evaluated.

Cite this: DOI: 10.1039/c0xx00000x

www.rsc.org/xxxxxx

ARTICLE TYPE

Lithium deposition on graphite anode during long-term cycles and the effect on capacity loss

Lijie Yang,[a] Xinqun Cheng,*[a] Yunzhi Gao,[a] Yulin Ma,[a] Pengjian Zuo,[a] Chunyu Du,[a] Yingzhi Cui,[a] Ting Guan,[a] Shuaifeng Lou,[a] Fuping Wang,[a] Weidong Fei[b] and Geping Yin*[a]

Received (in XXX, XXX) Xth XXXXXXXXX 20XX, Accepted Xth XXXXXXXXX 20XX
DOI: 10.1039/b000000x

Lithium deposition on the surface of graphite anode was evaluated using $LiCoO_2$/graphite battery during long-term cycles. The batteries were charged/discharged at 1C and 25 °C within the voltage range of 2.75~4.2 V for 600, 700, 800, 900 and 1000 cycles, respectively. Scanning electron microscopy (SEM) results indicated that both solid electrolyte interphase (SEI) film and lithium deposition appeared on the surface of cycled graphite anode. Dendritic and granular lithium deposition grew on the anode non-uniformly. Metallic lithium existed in the deposition according to differential scanning calorimeter (DSC) result. Capacity was declined distinctly from 800th cycle, corresponding to the growth of lithium deposition. SEI film was formed on the surface of lithium deposition. Results of X-ray photoelectron spectroscopy (XPS) test indicated that composition of SEI film on the surface of lithium deposition was the same as that of SEI film on the surface of cycled graphite. Capacity loss from electrolyte consumed by the formation of SEI film was 23.61%, while the loss from other battery components was 76.39%. Formation of lithium deposition consumed active lithium in the battery and led to capacity loss. According to test results of three-electrode cell, average anode potential at the end of constant-current charging for full battery became more negative with the cycling, and this phenomenon was related to the generation of lithium deposition.

Introduction

When $LiCoO_2$/graphite batteries were charged and discharged during the voltage range of 2.75~4.2 V, the known reasons leading to capacity loss were the continuous growth of solid electrolyte interphase (SEI) film on the surfaces of cathode[1,2] and anode,[3,4] the transformation of structures[5-8] and so on.

Cathode and anode may not be charged and discharged during the ideal voltage range sometimes though the full battery was cycled normally during 2.75~4.2 V. S.S. Zhang et al.[9] found that potential of graphite anode could be lower than 0 V (vs. Li^+/Li) during the constant-current charging of full battery. Therefore, it was possible for lithium to be deposited on the surface of graphite. The phenomenon may be more severe when the battery was charged at larger current or at lower temperature. The charging properties of batteries could be improved by increasing the capacity ratio of anode to cathode (A/C) appropriately. Mao-Sung Wu et al.[10] reported that the potential of mesocarbon microbead (MCMB) electrode decreased to -0.1 V (vs. Li^+/Li) during the charging when A/C was 0.9. Gray deposition appeared on the surface of fully charged MCMB, but it did not appear in the battery with A/C of 1.05. However, most of these studies focused on the effect of A/C on lithium deposition during the early stage of the cycling. If the deposition generated on the surface of carbon gradually during long-term charge/discharge cycles, the process would also affect capacity loss of the battery before leading to the safety problems,[11-13] which was not studied clearly at present. In this experiment, phenomenon of lithium deposition in long-term cycled battery, effect on capacity loss of battery and mechanism of formation were evaluated.

Experimental

The Li-ion battery used in this experiment was commercial cell with a nominal capacity of 1000 mAh. Cathode was prepared by coating the mixing slurry, which consisted of $LiCoO_2$, acetylene black, BP2000, polyvinylidene fluoride (PVDF) and a certain amount of N-methyl-2-pyrrolidinone (NMP), on aluminum foil. Anode consisted of graphite, Super-P, styrene-butadience rubber (SBR) and carboxymethyl cellulose (CMC), and electrolyte was 1 mol/L $LiPF_6$ dissolved in ethylene carbonate/diethyl carbonate/ethyl methyl carbonate (EC/DEC/EMC, 1:1:1 by volume). Vinylene carbonate (VC) and propylene sulfite (PS) as electrolyte additives were used in the commercial lithium ion battery. The batteries were charged and discharged at 0.2C firstly to obtain the capacity and then cycled at 1C for 600, 700, 800, 900 and 1000 times, respectively. Capacity verification of cycled batteries was conducted at 0.2C. All the charging and discharging were performed at 25 °C within the range of 2.75~4.2 V.

The cycled batteries were dismantled in the glove box filled with argon gas. The obtained anodes were immersed in dimethyl

carbonate (DMC) to remove the electrolyte $LiPF_6$. The morphology and composition of anodes were examined by scanning electron microscopy (SEM) and X-ray photoelectron spectroscopy (XPS). In order to avoid the exposure to air and moisture, the testing samples were sealed in argon-filled vessel and then transferred to SEM and XPS instruments. Atomic force microscopy (AFM) analysis was conducted on different areas of graphite anode cycled for 1000 times (Bruker Dimension Icon). The sample for differential scanning calorimeter (DSC, NETZSCH, STA 449 F3 Jupiter) analysis was obtained from the cycled graphite anode with the deposition and was sealed in a gold sample pan in the glove box. The heating temperature ranged from 30 °C to 230 °C and heating rate was 10 °C/min.

In order to examine the effect of cycled electrolyte on capacity loss, fresh electrolyte was added into cycled batteries and the obtained battery was charged and discharged at 0.2C to examine the capacity.

The cell after charge/discharge cycles was dismantled in the glove box and the obtained plate group including cathode, anode and separator were put into fresh electrolyte, along with the reference electrode (RE) of metal lithium plate. RE was close enough to anode and was isolated from anode by a layer of separator. The sealed three-electrode cell was shown in Fig. 1. Electrode potential of graphite anode (vs. Li^+/Li) was monitored when $LiCoO_2$/graphite battery was charged and discharged at 1C within the range of 2.75~4.2 V.

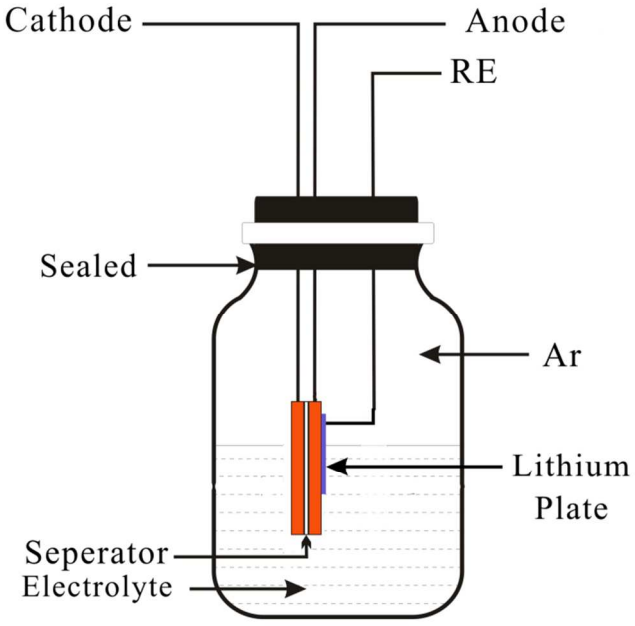

Fig. 1 Diagram of three-electrode cell of $LiCoO_2$/graphite battery.

Results and Discussion

$LiCoO_2$/graphite batteries were charged and discharged for 600, 700, 800, 900 and 1000 cycles at 1C, respectively. Capacity changing during 1000 cycles at 1C was demonstrated in Fig. 2 and capacity retention rates at 0.2C were shown in Table 1.

The capacity of $LiCoO_2$/graphite battery at 0.2C decreased with the cycling. Moreover, the capacity was declined obviously after the 800th cycle. This result indicated that obvious changes must have taken place inside the battery from the 800th cycle.

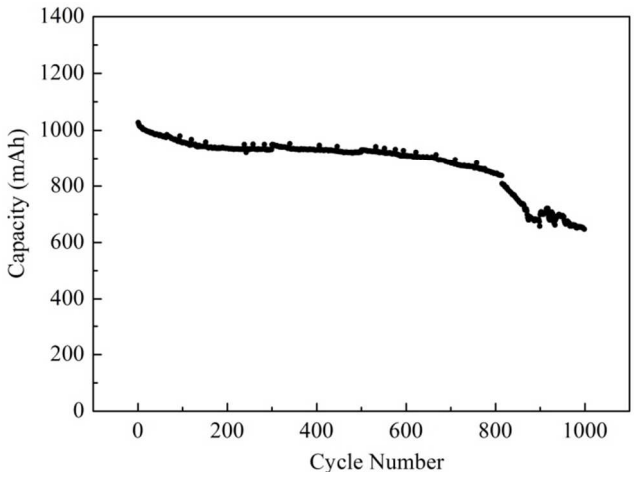

Fig. 2 Capacity changing of $LiCoO_2$/graphite battery during cycling at 1C.

Table 1 Capacity retention rates of $LiCoO_2$/graphite battery at 0.2C

Cycle number	Capacity retention rates at 0.2C（%）
600	86.96
700	82.66
800	74.80
900	76.71
1000	71.69

Fig. 3 showed SEM images of graphite electrodes after different cycles. The surfaces of pristine and activated electrodes were uniform, but some substances emerged after 600 and 700 cycles. The substances were fairly thick after 800 and 900 cycles, and covered a large proportion of the electrode after 1000 cycles. Therefore the growth of these substances with cycling was consistent with the changing of capacity. So capacity loss of the battery may be related with these substances on the surface of graphite. In addition, the substances on the surfaces of cycled electrodes were distributed unevenly.

It could be seen from Fig. 4a that pristine graphite was composed of graphite layers with clean surface. After 600 and 1000 cycles (Fig. 4c and f), two regions appeared on the surfaces of electrodes, one without deposition and the other with deposition. Membrane was formed on the surface of cycled graphite in the region without deposition (Fig. 4d and g), which could be postulated as SEI film.[14-16] The deposition was composed of dendritic and grainy material (Fig. 4b and e). The morphology of deposition was the same as that of lithium deposition in lithium batteries[17,18] and overcharged lithium ion batteries.[19,20] Morphologies of depositions on the electrodes after 600 and 1000 cycles were almost the same, but deposition layer on electrode cycled for 1000 times was thicker than that for 600 times (Fig. 4c and f).

Surface morphology of cycled graphite and lithium deposition could be examined by AFM. The surface of cycled graphite (Fig. 5a and c) was not flat, but large planes still existed. Rugged deposition (Fig. 5d) was composed of many protuberances with particle size of 0.7~2.2 μm (Fig. 5b and d). The deposition grew non-uniformly on the surface of graphite anode.

To verify the existence of metallic lithium on graphite anode

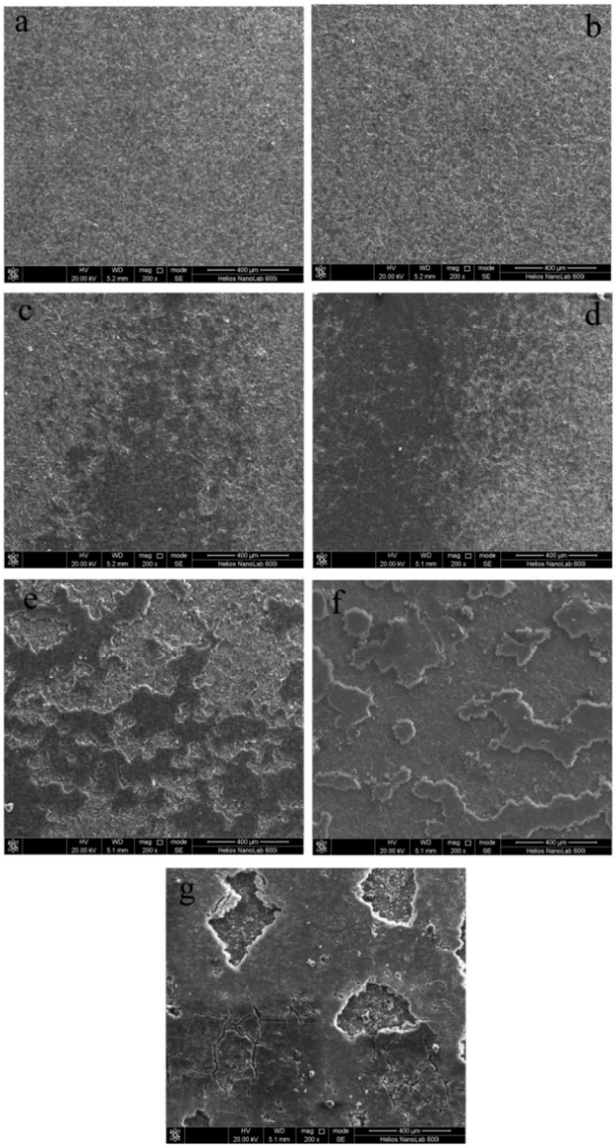

Fig. 3 SEM images of graphite electrodes after different cycles (a) pristine (b) activated (c) 600 cycles (d) 700 cycles (e) 800 cycles (f) 900 cycles (g) 1000 cycles.

after long-term cycles, DSC analysis was conducted on the cycled graphite anode with the deposition at fully charged state. The endothermic peak at 180 °C appeared in the DSC curve in Fig. 6 and it corresponded to the melting of metallic lithium.[21,22] Accordingly, metallic lithium surely existed in the deposition on the surface of long-term cycled graphite anode at charged state.

In order to examine surface compositions of the regions with and without deposition, XPS tests were performed on the two regions of graphite anode after 1000 cycles. XPS curves and fitting results of Li1s, C1s, O1s and F1s were shown in Fig. 7. Peaks at 56.2 eV and 54.2 eV in Li1s spectra could be attributed to LiF[23,24] and Li_2O,[25,26] respectively. The peak at 55.3 eV was assigned to Li_2CO_3,[27,28] LiOH[29,30] and $ROCO_2Li$.[29] In C1s spectra, peaks of C-C at 284.6 eV and C-H at 285.2 eV were from $ROCO_2Li$, $(-CH_2CH_2O-)_n$ (PEO) and ROLi. Peaks of C-O at 286.5 eV and CO_3^{2-} at 289 eV came from PEO, ROLi, $ROCO_2Li$ and Li_2CO_3. Peaks of Li-O-Li at 529.3 eV, Li-O-H and CO_3^{2-} at 531.9 eV, and C-O at 533.5 eV appeared in O1s spectra, which proved the formation of Li_2O, LiOH, $ROCO_2Li$, Li_2CO_3, PEO and ROLi.[31] Only peak of LiF at 686.2 eV[32] was observed in F1s spectra.

LiF, Li_2O, Li_2CO_3, LiOH, $ROCO_2Li$, ROLi and PEO appeared on the surfaces of both cycled graphite and deposition from the above results of XPS. Therefore SEI films were formed on the surfaces of both cycled graphite and lithium deposition. Peak positions in fitted Li1s, C1s, O1s and F1s spectra of the two regions were the same, which demonstrated that the composition of SEI film on the surface of lithium deposition was the same as that on the surface of cycled graphite.

The battery after certain cycles was dismantled and fresh electrolyte was added into the battery. Effect of cycled electrolyte on capacity loss of battery was examined by the charging and discharging at 0.2C. Charge/discharge curves of pristine battery, cycled battery and the cycled battery added fresh electrolyte were shown in Fig. 8. Shapes of the three charge/discharge curves were nearly the same.Capacity changes at 0.2C were shown in Table 2. Capacity retention rate of cycled battery was 82.62%, which meant capacity loss was 17.38%. The capacity appeared a slight recovery after fresh electrolyte being added into the cycled battery. The capacity retention rate returned to 86.72%, which demonstrated that the effect of battery components other than electrolyte on capacity loss was 13.28%. If the total capacity loss of 179.6 mAh after the cycling was defined as 100%, the capacity loss of 42.4 mAh (179.6 - 137.2 = 42.4) from electrolyte was 23.61% and the capacity loss from other components was 76.39%.

From XPS results, SEI film appeared on the surface of lithium deposition. Compositions of SEI film were reaction products of lithium deposition with electrolyte. Therefore, the appearance of lithium deposition led to the consumption of electrolyte. In addition, the formation of SEI film on the surfaces of graphite and $LiCoO_2$ electrodes could also consume electrolyte in the battery. These consumptions of electrolyte would decrease active lithium and ionic conductivity of battery, which was one of the reasons for capacity loss of the battery.

Table 2 Capacity changes at 0.2C of pristine battery, cycled battery and the cycled battery added fresh electrolyte

	Capacity at 0.2C (mAh)	Capacity retention rates at 0.2C (%)	Capacity loss (mAh)
pristine battery	1033.1	100.00	0
cycled battery	853.5	82.62	179.6
the cycled battery added fresh electrolyte	895.5	86.72	137.2

Lithium deposition itself also consumed active lithium of the battery. More deposition appeared on the anode with the cycling, so more active lithium were consumed, also leading to capacity loss of the battery.

The electrode potential of graphite anode during the charging and discharging of full battery was examined by three-electrode cell. Such experiments were conducted on two batteries after different cycles. Capacity retention rate of battery #1 was 97.78%, and that of #2 was 82.62%. These two batteries were charged and discharged at 1C. Voltage-time curves of full

batteries and their corresponding graphite anodes were shown in Fig. 9.

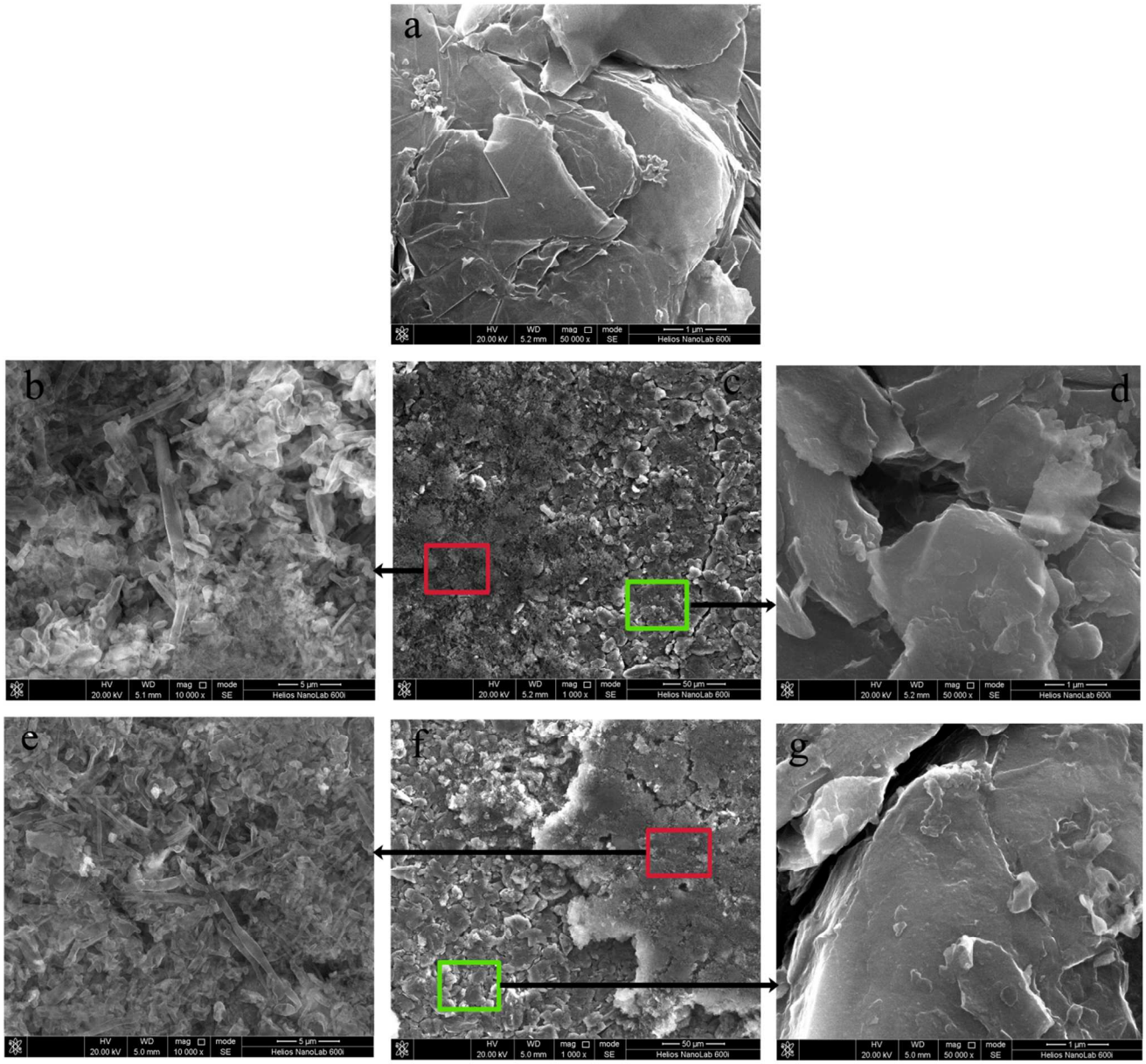

Fig. 4 SEM images of different regions on the surface of graphite electrodes after different cycles (a) pristine (b)(c)(d) 600 cycles (e)(f)(g) 1000 cycles.

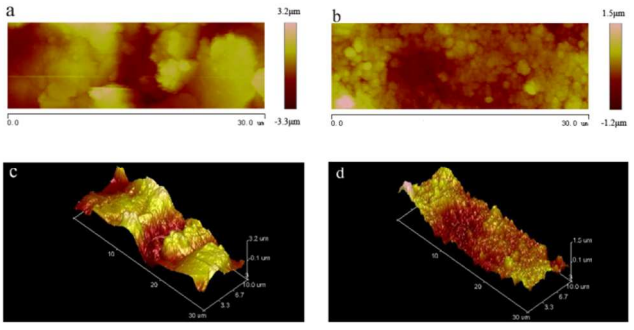

Fig. 5 AFM images of cycled graphite and lithium deposition (a) Two-dimensional height image of cycled graphite (b) Two-dimensional height image of lithium deposition (c) Three-dimensional height image of cycled graphite (d) Three-dimensional height image of lithium deposition.

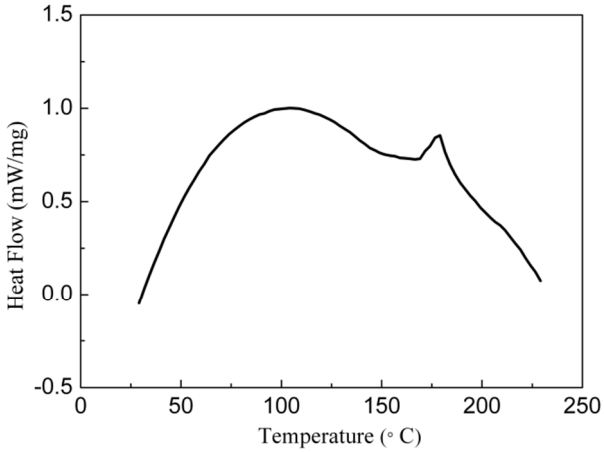

Fig. 6 DSC curve of the cycled graphite anode at fully charged state.

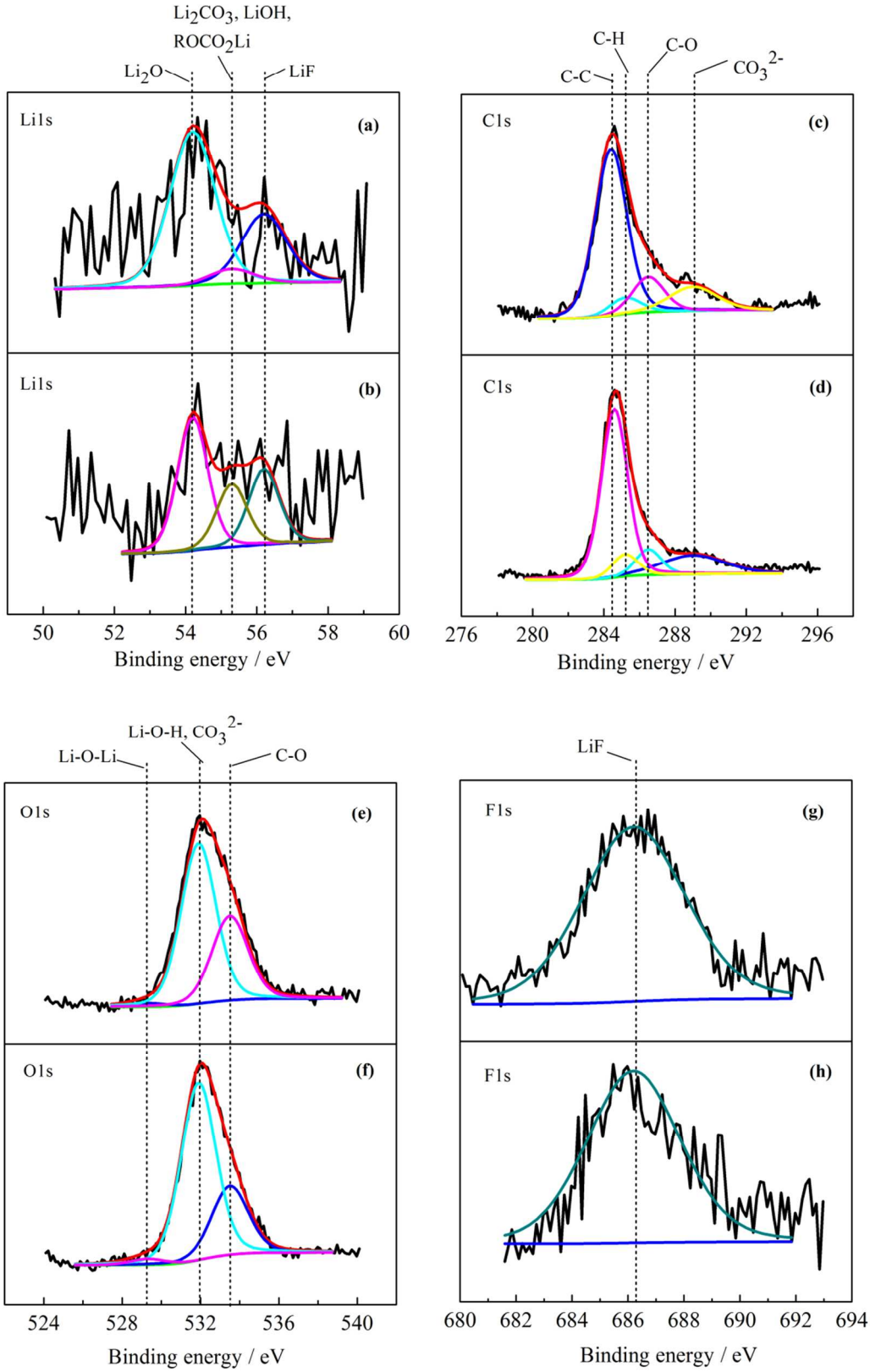

Fig. 7 XPS curves and fitting results of Li1s, C1s, O1s and F1s in the regions with and without depositions on the surface of graphite electrodes after 1000 cycles(a)(c)(e)(g) the region with depositions (b)(d)(f)(h) the region without depositions.

The charge/discharge voltage ranges of graphite anodes were during the range of 0.09~0.19 V. For the charging process of full

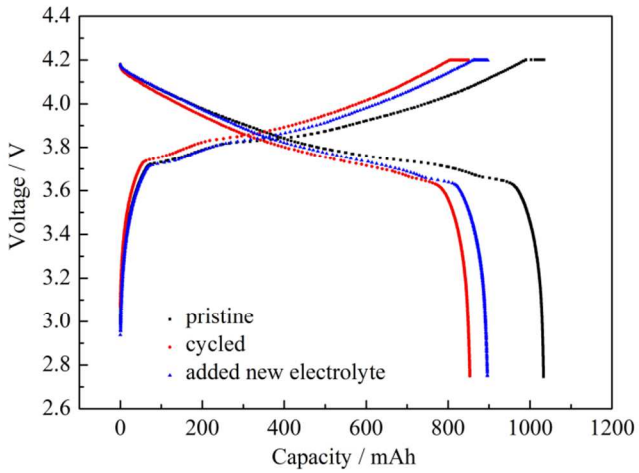

Fig. 8 Charge/discharge curves at 0.2C of pristine battery, cycled battery and the cycled battery added fresh electrolyte.

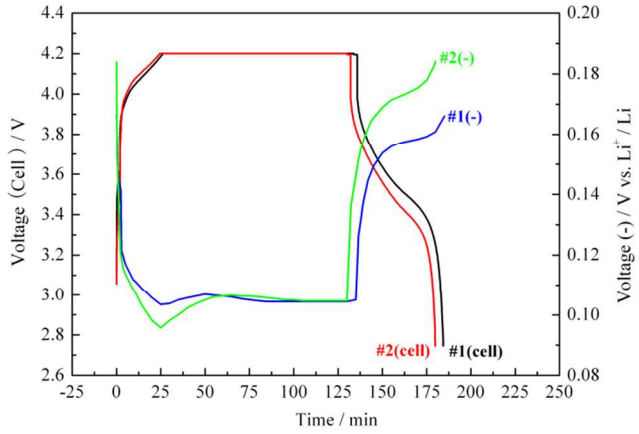

Fig. 9 Voltage-time curves of full batteries #1, #2 and corresponding graphite anodes during the charging and discharging of the two batteries at 1C.

battery, anode potential decreased continuously during constant-current charging, and then increased slightly during the following constant-voltage charging. Therefore the lowest anode potential appeared at the end of constant-current charging of full battery. The lowest anode potential of #1 was 0.103 V and that of #2 was 0.096 V, which indicated that the lowest anode potential of #2 was more negative than that of #1. The measured anode potential by three-electrode cell was average potential of the whole graphite anode. Maybe local potential of the cycled anode was below 0 V (vs. Li^+/Li), leading to the deposition of lithium metal. Because lithium depositions in #2 were more than those in #1, average potential of #2 at the end of constant-current charging was more negative than that of #1.

Conclusions

Lithium deposition was evaluated using $LiCoO_2$/graphite batteries during long-term cycles. The batteries were charged and discharged at the rate of 1C within the voltage range of 2.75~4.2 V for 600, 700, 800, 900 and 1000 cycles, respectively. Capacity was declined obviously from 800th cycle, which was consistent with the change of surface morphology of graphite anode. As the cycle proceeding, more lithium deposition was also formed on the surface of graphite besides SEI film. The dendritic and granular deposition distributed non-uniformly. DSC result verified the existence of metallic lithium in the deposition. SEI film was also formed on the surface of lithium deposition. The components were the same as those of SEI film on the surface of graphite, which were LiF, Li_2O, Li_2CO_3, LiOH, $ROCO_2Li$, ROLi and PEO. Formation of these surface films would consume the electrolyte in the battery. Capacity loss from electrolyte was 23.61%, while capacity loss from other battery components was 76.39%. In addition, the formation of lithium deposition also consumed active lithium and caused capacity loss. Local potential of graphite anode below 0 V led to the generation of lithium deposition, making the average anode potential at the end of constant-current charging for full battery more negative during the cycling.

Acknowledgements

The authors would like to thank the financial support from the National High Technology Research and Development Program (863 Program) of China (No. 2012AA110203).

Notes and references

[a] *Institute of Advanced Chemical Power Sources, School of Chemical Engineering and Technology, Harbin Institute of Technology, Harbin 150001, China. Fax: +86-451-86413717; Tel: +86-451-86413707; E-mail: chengxq@hit.edu.cn ; yingeping@hit.edu.cn*
[b] *School of Materials Science and Engineering, Harbin Institute of Technology, Harbin 150001, China.*

1. Y. Takanashia, Y. Orikasaa, M. Mogia, M. Oishia, H. Murayamaa, K. Satoa, H. Yamashigea, D. Takamatsua, T. Fujimotoa, H. Tanidaa, H. Araia,T. Ohtab, E. Matsubarac, Y. Uchimotod and Z. Ogumia, *J. Power Sources*, 2011, **196**, 10679.
2. M. Jo, Y.-S. Hong, J. Choo and J. Cho, *J. Electrochem. Soc*., 2009, **156**, A430.
3. J.T. Lee, N. Nitta, J. Benson, A. Magasinski, T.F. Fuller and G. Yushin, *Carbon*, 2013, **52**, 388.
4. M. Lu, H. Cheng and Y. Yang, *Electrochim. Acta*, 2008, **53**, 3539.
5. X. Wang, Y. Sakiyama, Y. Takahashi, C. Yamada, H. Naito,G. Segami, T. Hironaka, E. Hayashi and K. Kibe, *J. Power Sources*, 2007, **167**, 162.
6. H.P. Zhang, L.J. Fu, Y.P. Wu and H.Q. Wu, *Electrochem. Solid-State Lett*., 2007, **10**, A283.
7. C.-N. Li, J.-M. Yang, V. Krasnov, J. Arias and K.-W. Nieh, *Electrochem. Solid-State Lett*., 2008, **11**, A81.
8. P.L. Moss, G. Au, E.J. Plichta and J.P. Zhenga, *J. Electrochem. Soc*., 2010, **157**, A1.
9. S.S. Zhang, K. Xu and T.R. Jow, *J. Power Sources*, 2006, **160**, 1349.
10. M.-S. Wu, P.-C.J. Chiang and J.-C. Lin, *J. Electrochem. Soc*., 2005, **152**, A47.
11. F. Ding, W. Xu, G.L. Graff, J. Zhang, M.L. Sushko, X. Chen, Y. Shao, M.H. Engelhard, Z. Nie, J. Xiao, X. Liu, P.V. Sushko, J. Liu and J.-G. Zhang, *J. Am. Chem. Soc*., 2013, **135**, 4450.
12. G. Park, N. Gunawardhana, H. Nakamura, Y.-S. Lee and M. Yoshio, *J. Power Sources*, 2012, **199**, 293.
13. P. Arora, M. Doyle and R.E. White, *J. Electrochem. Soc*., 1999, **146**, 3543.
14. H. Buqa, A. Würsig, J. Vetter, M.E. Spahr, F. Krumeich and P. Novák, *J. Power Sources*, 2006, **153**, 385.
15. P. Verma, P. Maire and P. Novák, *Electrochim. Acta*, 2010, **55**, 6332.
16. M. Kassem and C. Delacourt, *J. Power Sources*, 2013, **235**, 159.
17. K. Kanamura, H. Tamura, S. Shiraishi and Z. Takehara, *J. Electroanal. Chem*., 1995, **394**, 49.
18. C.M. López, J.T. Vaughey and D.W. Dees, *J. Electrochem. Soc*., 2012, **159**, A873.

19. W. Lu, C.M. López, N. Liu, J.T. Vaughey, A. Jansen and D.W. Dees, *J. Electrochem. Soc*., 2012, **159**, A566.
20. D. Belov and M.-H. Yang, *J. Solid State Electrochem*., 2008, **12**, 885.
21. H. Maleki, G. Deng, A. Anani and J. Howard, *J. Electrochem. Soc*., 1999, **146**, 3224.
22. T. Kawamura, A. Kimura, M. Egashira, S. Okada and J.-I. Yamaki, *J. Power Sources*, 2002, **104**, 260.
23. K. Kanamura, H. Tamura, S. Shiraishi and Z.-I. Takehara, *J. Electroanal. Chem*., 1995, **394**, 49.
24. D. Aurbach, I. Weissman, A. Schechter and H. Cohen, *Langmuir*, 1996, **12**, 3991.
25. K. Kanamura, S. Shiraishi, H. Tamura and Z.-I. Takehara, *J. Electrochem. Soc*., 1994, **141**, 2379.
26. K. Edström, M. Herstedt and D.P. Abraham, *J. Power Sources*, 2006, **153**, 380.
27. K.-I. Morigaki and A. Ohta, *J. Power Sources*, 1998, **76**, 159.
28. A.M. Andersson, A. Henningson, H. Siegbahn, U. Jansson and K. Edström, *J. Power Sources*, 2003, **119-121**, 522.
29. D. Bar-Tow, E. Peled and L. Burstein, *J. Electrochem. Soc*., 1999, **146**, 824.
30. K. Kanamura,H. Tamura and Z. Takehara, *J. Electroanal. Chem*., 1992, **333**, 127.
31. L. Yang, X. Cheng, Y. Ma, S. Lou, Y. Cui, T. Guan and G. Yin, *J. Electrochem. Soc*., 2013, **160**, A2093.
32. V. Eshkenazi, E. Peled, L. Burstein and D. Golodnitsky, *Solid State Ionics*, 2004, **170**, 83.